JBC Papers in Press. Published on January 13, 2010 as Manuscript M109.074161
The latest version is at http://www.jbc.org/cgi/doi/10.1074/jbc.M109.074161

STRUCTURAL AND FUNCTIONAL CHARACTERIZATION OF A NOVEL HOMODIMERIC THREE-FINGER NEUROTOXIN FROM THE VENOM OF *OPHIOPHAGUS HANNAH* (KING COBRA)

Amrita Roy[1]; Xingding Zhou[1]; Ming Zhi Chong[1]; Dieter D'hoedt[2]; Chun Shin Foo[1]; Nandhakishore Rajagopalan[1,3]; Selvanayagam Nirthanan[4,5]; Daniel Bertrand[2]; J Sivaraman[1] and R. Manjunatha Kini[1,6*]

[1] Department of Biological Sciences, National University of Singapore, Singapore 117543
[2] Department of Neuroscience, Medical Faculty, University of Geneva, 1211 Geneva 4, Switzerland
[3] Current address: ZMBH, University of Heidelberg, 69120 Heidelberg, Germeny
[4] School of Medical Science, Griffith University Gold Coast Campus, Queensland 4131, Australia
[5] Department of Pharmacology, School of Medicine, National University of Singapore, Singapore 117597
[6] Department of Biochemistry and Molecular Biophysics, Medical College of Virginia, Virginia Commonwealth University, Virginia 23298, USA

Running head: Haditoxin, the first dimeric α-neurotoxin

[*] To whom correspondence may be addressed: R. Manjunatha Kini, Protein Science Laboratory, Department of Biological Sciences, Faculty of Science, National University of Singapore, Singapore 117543; Tel. 65-6516-5235; Fax. 65-6779-2486; E-Mail: dbskinim@nus.edu.sg

Snake venoms are a cocktail of pharmacologically active proteins and polypeptides which have led to the development of molecular probes and therapeutic agents. Here, we describe the structural and functional characterization of a novel neurotoxin, Haditoxin from the venom of *Ohiophagus hannah* (King cobra). Haditoxin exhibited novel pharmacology with antagonism towards muscle (αβγδ) and neuronal (α_7, $\alpha_3\beta_2$ and $\alpha_4\beta_2$) nicotinic acetylcholine receptors (nAChRs), with highest affinity for α_7-nAChRs. The high resolution (1.5 Å) crystal structure revealed haditoxin to be a homodimer, like κ-neurotoxins which target neuronal $\alpha_3\beta_2$- and $\alpha_4\beta_2$-nAChRs. Interestingly however, the monomeric subunits of haditoxin were composed of a three-finger protein fold typical of curaremimetic short-chain α-neurotoxins. Biochemical studies confirmed that it existed as a non-covalent dimer species in solution. Its structural similarity to short-chain α-neurotoxins and κ-neurotoxins notwithstanding, haditoxin exhibited unique blockade of α_7-nAChRs (IC_{50} 180 nM), which is recognized by neither short-chain α-neurotoxins nor κ-neurotoxins. This is the first report of a dimeric short-chain α-neurotoxin interacting with neuronal α_7-nAChRs as well as the first homodimeric three-finger toxin to interact with muscle nAChRs.

Snake venoms are a rich source of pharmacologically active proteins and polypeptides targeting a variety of receptors with high affinity and specificity (1). Because of their high specificity, some of these molecules have contributed significantly, (a) to the isolation and characterization of different receptors and their subtypes in the field of molecular pharmacology, and (b) as lead compounds in the development of therapeutic agents (2;3). For example, the discovery of α-bungarotoxin, a postsynaptic neurotoxin from the venom of *Bungarus multicinctus* led to the identification of the nicotinic acetylcholine receptor (nAChR) – the first isolated receptor protein (4) as well as the first one to characterized electrophysiologically (5) and biochemically (6;7). Subsequently, it was also used to characterize several other nAChRs (8-10).

Snake venom proteins can be broadly classified as enzymatic and non-enzymatic proteins. Three-finger toxins (3FTxs) are the largest group of non-enzymatic snake venom proteins (1;11). They are most commonly found in the venoms of elapid and hydrophiid snakes. Recently, our laboratory has also demonstrated the presence of 3FTxs from colubrid venoms (12;13) and 3FTx transcripts have been found in the venom gland transcriptome of viperid snakes (14;15). The proteins in this family of toxins share a common structural scaffold of three β-sheeted

loops emerging from a central core (11;16). Despite the overall similarity in structure, these proteins have diverse functional properties. Members of this family include neurotoxins targeting the cholinergic system (7;11;16), cytotoxins/cardiotoxins interacting with the cell membranes (17), calciseptine and related toxins that block the L-type Ca^{2+} channels (18), dendroaspins, which are antagonists of various cell-adhesion processes (19) and β-cardiotoxin antagonizing the β-adrenoceptors (20). The subtle variations in their structures, such as the presence of extra disulfide bonds, differences in size and overall conformation (twists and turns) of the loops and longer C-terminal and/or N-terminal extensions (21), may contribute to the observed functional diversity as well as specificity of these toxins (22).

This family contains several types of neurotoxins that interact with different subtypes of nicotinic and muscarinic receptors involved in central and peripheral cholinergic transmission. Depending on the target receptors, these neurotoxins can be broadly divided into various groups. Curaremimetic or α-neurotoxins that target muscle (αβγδ or α_1 subtype) nAChRs (7;16;23) belong to short-chain and long-chain neurotoxins (classified based on size and number of disulfide bridges; (24)). Long-chain neurotoxins, but not short-chain neurotoxins, also target neuronal α_7-nAChRs associated with neurotransmission in the brain (25). κ-Neurotoxins, such as κ-bungarotoxin (*Bungarus multicinctus*) show specificity for other neuronal subtypes, $\alpha_3\beta_2$- and $\alpha_4\beta_2$-nAChRs (26;27). Muscarinic 3FTxs, unlike many small molecule ligands, can distinguish between different types of muscarinic acetylcholine receptors (mAChRs) [For review see, (28)], and hence are useful in the characterization of these receptor subtypes. Muscarinic toxin1, isolated from the venom of *Dendroaspis angusticeps* interacts with mAChR subtype1 (M1) (29), whereas muscarinic toxin 3 (MT3), isolated from the same snake interacts with M4 mAChRs (30). In recent years, new 3FTxs with distinct and novel receptor specificities have been characterized and added to this growing library (12;13;31-36) justifying their usefulness as pharmacological tools to dissect the cholinergic circuitry to understand the role of individual receptor subtypes or offer clues to the rational design of specific therapeutics.

All neurotoxins characterized to date exist as monomers with the exception of κ-neurotoxins from *Bungarus sp.* (37;38), which is a non-covalently linked homodimer that binds neuronal ($\alpha_3\beta_2$ and $\alpha_4\beta_2$), but not muscle (αβγδ) nAChRs. More recently, we published the first report of a covalent heterodimeric neurotoxin, irditoxin from the venom of *Boiga sp.* which was a uniquely irreversible inhibitor of muscle (αβγδ) nAChRs (13). Here we report the purification, pharmacological characterization and a high resolution crystal structure of a novel non-covalent homodimeric neurotoxin from the venom of *Ophiophagus hannah* (King cobra). Although its quaternary structure is similar to κ-neurotoxins, it exhibited novel pharmacology with potent blocking activity on muscle (αβγδ) as well as neuronal (α_7, $\alpha_3\beta_2$ and $\alpha_4\beta_2$) nAChRs. Based on the high resolution crystal structure (1.55 Å) we have explored its structural similarities with other neurotoxins. This new toxin was named Haditoxin (*O. hannah* dimeric neurotoxin), and is the first homodimeric three-finger neurotoxin interacting with α_1-nAChRs.

Experimental procedures

Materials

Lyophilized *O. hannah* venom was obtained from PT Venom Indo Persada (Jakarta, Indonesia) and Kentucky Reptile Zoo (Slade, KY, USA). Reagents for N-terminal sequencing by Edman degradation are from Applied Biosystems (Foster City, CA, USA). Potassium chloride (KCl), acetonitrile (ACN) and trifluoroacetic acid (TFA) were from Merck KGaA, Darmstadt, Germany. Precision Plus Protein Standards, dual color (marker for SDS-PAGE) and Bis(sulfosuccinimidyl) suberate (BS^3) were purchased from Bio-Rad Laboratories (Hercules, CA, USA) and Pierce (Rockford, IL, USA) respectively. Superdex 30 Hiload (16/60) column and Jupiter C18 (5 μ, 300 Å, 4.6 mm x 150 mm) were purchased

from GE Healthcare Life Sciences (Piscataway, NJ, USA) and Phenomenex (Torrance, CA, USA) respectively. Crystal screening solution and accessories were obtained from Hampton Research (Aliso Viejo, CA, USA). All other chemicals including α-bungarotoxin from *Bungarus multicinctus* were purchased from Sigma-Aldrich (St. Louis, MO, USA). All the reagents were of the highest purity grade. Water was purified using a MilliQ system (Millipore, Billerica, MA, USA).

Animals

Animals (Swiss albino mice and Sprague Dawley rats) were acquired from the National University of Singapore Laboratory Animal Center and acclimatized to the Department's Animal Holding Unit for at least 3 days before the experiments. They were housed, four per cage, with food and water available *ad libitum* in a light controlled room (12 h light/dark cycle, light on at 0700 h) at 23 °C and 60% relative humidity. Domestic chicks (*Gallus domesticus*) were purchased from Chew's Agricultural Farm, Singapore and delivered on the day of experimentation. Animals were sacrificed by exposure to 100% carbon dioxide. All experiments were conducted according to the Protocol (021/07a) approved by the Institutional Animal Care and Use Committee of the National University of Singapore.

Purification of the protein

O. hannah crude venom (100 mg dissolved in 1 ml of MilliQ water and filtered) was loaded onto a Superdex 30 gel filtration column, equilibrated with 50 mM Tris-HCl buffer; pH 7.4 and eluted with the same buffer using an ÄKTA purifier system (GE Healthcare Life Sciences, Piscataway, NJ, USA). Fractions containing the toxin of interest were further sub-fractionated by reverse phase-high performance liquid chromatography (RP-HPLC) using a Jupiter C18 column, equilibrated with 0.1% (v/v) TFA and eluted with a linear gradient of 80% (v/v) ACN in 0.1% (v/v) TFA. Elution was monitored at 280 and 215 nm. Fractions were directly injected into an API-300 LC/MS/MS system (PerkinElmer Life Sciences, Wellesley, MA, USA) to determine the mass and homogeneity of the protein as described previously (20). Analyte software (PerkinElmer Life Sciences, Wellesley, MA, USA) was used to analyze and deconvolute the raw mass data. Fractions showing the expected molecular mass were pooled and lyophilized.

Capillary electrophoresis

Capillary electrophoresis was performed on a BioFocus3000 system (Bio-Rad, Hercules, CA, USA) to determine the homogeneity of the protein after RP-HPLC. The native protein (1 µg/µl) was injected to a 25 µm x 17 cm coated capillary using a pressure mode (5 p.s.i./s) and run in 0.1 M phosphate buffer (pH 2.5) under 18 kV at 20 °C for 7 min. The migration was monitored at 200 nm.

N-terminal sequencing

N-terminal sequencing of the native protein was performed by automated Edman degradation using a Procise 494 pulsed-liquid-phase protein sequencer (Applied Biosystems, Foster City, CA, USA) with an on-line 785A phenylthiohydantion (PTH)-derivative analyzer. The PTH amino acids were sequentially identified by mapping the respective separation profiles with the standard chromatogram.

Circular dichroism (CD) spectroscopy

Far-UV CD spectra (260-190 nm) were recorded using a Jasco J-810 spectropolarimeter (Jasco Corporation, Tokyo, Japan) as described previously (20). The protein samples (concentration range 0.25-1 mg/ml) were dissolved in MilliQ water.

***In vivo* toxicity study**

Native protein (200 µl dissolved in 0.89% NaCl) was injected intra-peritoneally (*i.p.*) using a $27_G1/2$" needle (Becton-Dickinson, Franklin Lakes, NJ, USA) into male Swiss albino mice (15 ± 2 g) at doses of 5, 10 and 25 mg/kg (n = 2). The symptoms of envenomation were observed, and in the event of death, the time of death was noted. Control group was injected with 200 µl of 0.89% NaCl.

Postmortem examinations were conducted on all animals.

***Ex vivo* organ bath studies**

Isolated tissue experiments were performed as previously described (13;31) using a conventional organ bath (6 ml) containing Krebs solution of the following composition (in mM): 118 NaCl, 4.8 KCl, 1.2 KH_2PO_4, 2.5 $CaCl_2$, 25 $NaHCO_3$, 2.4 $MgSO_4$, and 11 D-(+) glucose); pH 7.4, at 37 ^oC. This is continuously aerated with carbogen (5% carbon dioxide in oxygen). The resting tension of the tissues was maintained at 1-2 g and the preparations were allowed to equilibrate for 30-45 min. Electrical field stimulation (EFS) was carried out through platinum ring electrodes using a Grass stimulator S88 (Grass Instruments, West Warwick, RI, USA). The magnitude of the contractile response was measured in gram (g) tension. Data was continuously recorded on PowerLab/Chart 5 data acquisition system via a force displacement transducer (Model MLT0201) (AD Instruments, NSW, Australia). Neuromuscular blockade produced by a toxin is expressed as a percentage of the original twitch height in the absence of exposure to toxin. Dose-response curves representing the percent blockade after 30 min of exposure to the respective toxins were plotted.

Chick biventer cervicis muscle (CBCM) preparations

The CBCM nerve-skeletal muscle preparation (39) was isolated from chicks (6 to 10 days old) and mounted in the organ bath chamber, under similar experimental conditions as described previously (12;31). The effect of haditoxin (0.05-5 μM; n = 3) or α-bungarotoxin (0.01-1.0 μM; n = 3) on nerve-evoked twitch responses of the CBCM were studied. In separate experiments, the recovery from complete neuromuscular blockade was assessed by washing out the toxin with Krebs solution, at 30 min intervals (3 cycles of 30 s on - 30 s off pulse) over a 120 min period.

Rat hemidiaphragm muscle (RHD) preparations

The RHD muscle associated with the phrenic nerve (40) was isolated and mounted in a 5-ml organ bath chamber, under similar conditions as stated for CBCM, as described previously (13). The effects of haditoxin (0.15-15 μM; n = 3) or α-bungarotoxin (0.01-1.0 μM; n = 3) on nerve-evoked twitch responses of the RHD were investigated. Recovery of neuromuscular blockade was assessed similarly as described above for CBCM.

Electrophysiogy

Two-electrode voltage-clamp (TEVC) experiments were done using *Xenopus* oocytes. The oocytes were prepared and injected as described by Hogg et al, (41). Briefly, 2 ng of cDNA encoding for human $\alpha_4\beta_2$-, $\alpha\beta\delta\varepsilon$-, α_7- and $\alpha_3\beta_2$-nAChRs were injected into the oocytes. TEVC measurements were done 2-3 days after injection. During recordings, the oocytes were perfused with OR2 (oocyte ringer) containing (in mM): 82.5 NaCl, 2.5 KCl, 1 $MgCl_2$, 2.5 Ca_2Cl, 5 HEPES, and 20 μg/ml BSA; pH 7.4. Atropine (0.5 μM) was added to all solutions to block activity of endogenous muscarinic receptors. Just before use, acetylcholine (ACh) and haditoxin were dissolved the OR2 solution. All recordings were performed with an automated TEVC robot. Oocytes were clamped at –100 mV and data were digitized and analyzed off-line using MATLAB (Mathworks, Natick, MA).

Gel filtration chromatography

The oligomeric states of the protein were examined by gel filtration chromatography on a Superdex 75 column (1 cm x 30 cm) equilibrated with 50 mM Tris-HCl buffer (pH 7.4) using an ÄKTA purifier system at a flow rate of 0.6 ml/min. Calibration was done using bovine serum albumin (66 kDa), carbonic anhydrase (29 kDa), cytochrome C (12.4 kDa), aprotinin (6.5 kDa) and blue dextran (200 kDa) as molecular weight markers. Native protein (0.25-10 μM) as well as samples (0.25-10 μM) treated 0.6% sodium dodecyl sulfate (SDS) (2 h of incubation at room temperature) (37) were loaded separately onto the column and respective elution profiles were recorded. For the SDS treated samples

the column was equilibrated with the same buffer containing 0.1% SDS.

Electrophoresis

Tris-Tricine SDS-PAGE of the protein of interest in the presence or absence of cross-linker BS^3 (42) was performed on a 12% gel, under reducing conditions, using Bio-Rad Mini-Protean II electrophoresis system. The concentration of BS^3 used was 5 mM. The protein bands were visualized by Coomassie Blue staining.

Crystallization and data collection

Crystallization conditions for the protein were screened with Hampton Research screens using hanging-drop vapor-diffusion method. Lyophilized protein was dissolved in 10 mM Tris-HCl buffer pH 7.4 with 100 mM NaCl. Crystallization experiments were performed at room temperature 297 K (24 °C), with drops containing equal volumes (1 µl) of reservoir and protein solution. Small rod-shaped crystals were formed within 2-3 days and grew to diffraction quality after three weeks. They were briefly soaked in the reservoir solution supplemented with 10% glycerol as cryo-protectant, prior to the X-ray diffraction data collection. Then these were flash-frozen in a nitrogen cold stream at 100 K (-173 °C). Diffraction up to 1.55 Å was obtained using a CCD detector (Platinum135) mounted on a Bruker Microstar Ultra rotating anode generator (Bruker AXS, Madison, WI, USA). A complete data set was collected, processed and scaled using the program HKL2000 (43).

RESULTS

Five novel 3FTxs were identified from the cDNA library of the venom gland tissue of *O. hannah* and one of them, named β-cardiotoxin, has been characterized previously (20). Here we describe the characterization of the second novel toxin, identified previously as MTLP-3 homolog based on sequence homology (20) **(Fig. 1)**. The LC/MS profile of *O. hannah* venom (44) showed the presence of a 7,535.67 ± 0.60 Da protein, similar to the expected molecular weight of the protein being characterized. This protein was purified from the crude venom using a two-step chromatographic approach. Firstly, the venom components were separated based on their sizes into five peaks using gel filtration chromatography **(Fig. 2A)**. Subsequently, each peak was fractionated by RP-HPLC and the fractions were analyzed by ESI-MS to identify the presence of the protein of interest (marked by a black bar in **Fig. 2A**). Further, these fractions were pooled and separated by RP-HPLC **(Fig. 2B)**. The ESI-MS of fraction 2a (indicated by a black arrow in **Fig. 2C**) showed three peaks with mass/charge (m/z) ratios ranging from +4 to +6 charges **(Fig. 2C)**, and the final reconstructed mass spectrum showed a molecular weight of 7535.67 ± 1.25 Da, which matched the calculated mass of 7534.42 Da **(Fig. 2C, inset)**. The secondary structural elements of haditoxin were analyzed using far-UV CD spectroscopy. The spectrum shows maxima at 230 nm and 198-200 nm and a minimum at 215 nm **(Fig. 2D)**. Thus haditoxin was found to be composed of β-sheeted structure similar to all other 3FTxs (11;16). The presence of a single protein peak in the electropherogram **(Fig. 2E)** indicates the homogeneity of the protein, ensuring the absence of contaminants, especially other α-neurotoxin(s) and cytotoxins present in the venom. Identification was further confirmed by N-terminal sequencing of the first 36 residues which matched the cDNA sequence of MTLP-3 homolog (20). This protein was found to be a homodimer (see below) and hence was renamed as haditoxin (*O. hannah* dimeric toxin) following the nomenclature of dimeric 3FTxs (12;13).

Investigation of haditoxin for muscarinic effects

As detailed in **Fig. 1A and B**, haditoxin showed high similarity (80-83%) with muscarinic toxin homologs (MTLP and MTLP-3) as well as similarity with muscarinic toxins (MT-α, MT7 and MT3) (51-52%). As such, we examined the effects of haditoxin on in vitro smooth muscle preparations, the rat ileum and rat anococcygeus muscle, pharmacologically characterized to represent M2 (45) and M3 mAChRs (46), respectively. In both preparations, the protein had no effect

on the contractile response of the muscle to exogenously applied ACh or EFS, suggesting that haditoxin does not interact with M2 and M3 mAChRs (Supplementary Figure S1). Therefore, it is likely that the observed sequence similarity with muscarinic toxin homologs is probably coincidental due to either phylogeny or structure, including the presence of the core disulfide bridges, and not the function. This merits further investigation, including electrophysiological studies and/or binding assays on other subtypes of mAChRs.

***In vivo* toxicity of haditoxin**

In preliminary experiments to observe the biological effects of haditoxin, all mice injected with the toxin (5, 10 and 25 mg/kg) showed typical symptoms of peripheral neurotoxicity, such as paralysis of hind limbs and labored breathing, and finally died, presumably due to respiratory paralysis (47;48). The time of death was recorded for each animal, with the average calculated to be 94, 32.5 and 20 min, respectively for the 5, 10 and 25 mg/kg doses. On post-mortem, no gross changes in the internal organs, notably hemorrhage, was observed.

***Ex vivo* neurotoxic effects of haditoxin**

The observed peripheral neurotoxic symptoms produced by haditoxin *in vivo*, warranted detailed pharmacological characterization on neuromuscular transmission using CBCM and RHD preparations. Haditoxin (1.5 μM) produced a reproducible time- and dose-dependent neuromuscular blockade in both the preparations **(Fig. 3A and 3C)**. In the CBCM, it completely inhibited the contractile response to exogenous agonists (ACh and CCh), whereas response to exogenous KCl and twitches evoked by direct muscle stimulation were not inhibited, indicating a post-synaptic neuromuscular blockade and an absence of direct myotoxicity.

The IC_{50} of haditoxin on CBCM and RHD was 0.27 ± 0.07 μM and 1.85 ± 0.39 μM respectively **(Fig. 3E)** (considering the fact that the protein exists as dimer in solution; see below). Compared to α-bungarotoxin (IC_{50} on CBCM 12.1 ± 5.4 nM and RHD 100.5 ± 22.5 nM) **(Fig. 3E)**, haditoxin was about 50 times less potent on both avian (CBCM) and mammalian (RHD) neuromuscular junctions. Reversibility of the neuromuscular blockade was tested for both the preparations with intermittent washing (indicated by black arrows in figure 3D and 3F). Partial recovery of the contractile response (60% recovery in 2 h) was observed in the CBCM **(Fig. 3B)** but not in the RHD **(Fig. 3D)**. These results indicate that, unlike typical α-neurotoxins like α-bungarotoxin, haditoxin exhibits partial reversibility in action, at least in the CBCM.

Effect of haditoxin on human nAChRs

Since haditoxin blocked the muscle activity of the CBCM and RHD, we examined its activity on human αβδε-nAChRs. Haditoxin completely inhibited the ACh-induced αβδε currents at a concentration of 10 μM **(Fig. 4A)**, with an IC_{50} value was 550 nM (n=13) **(Fig. 4B)**. This inhibition was practically irreversible within 8 min washout. This result is in good agreement with the findings on e*x vivo* studies with RHD as discussed earlier. Next, we tested the activity of haditoxin on α_7- and $\alpha_3\beta_2$-nAChRs. On α_7-nAChRs an irreversible block was observed at 10 μM concentration of haditoxin **(Fig 4C)** with an IC_{50} value was 180 nM (n=4) **(Fig 4D)**. As shown in **Fig. 4E**, 10 μM haditoxin fully blocked the response of $\alpha_3\beta_2$-nAChRs, with an IC_{50} value of 500 nM (n=4) **(Fig. 4F)**. Notably the blockade at $\alpha_3\beta_2$ was fully reversible whereas long lasting blockade was observed at α_7-nAChRs. This suggests that the K_{Off} value at the α_7 receptor is much smaller than at $\alpha_3\beta_2$-nAChRs. As these two receptors display about equivalent IC_{50}'s, this indicates that their respective K_{On} values are probably significantly different. However, the experimental protocol used herein prevents the detailed analysis of the K_{On} and K_{Off} values. An additional difference between these two receptors resides in their structural composition. While it is thought that α_7-nAChRs display five identical ligand binding sites, only two binding sites are proposed for the $\alpha_3\beta_2$-nAChRs. The difference in number of binding sites and effects on competitive

blockade was previously discussed for α_7- and $\alpha_4\beta_2$-nAChRs showing significant functional outcomes (49). Interestingly, haditoxin was almost 3-fold more potent to block ACh-induced responses mediated by α_7- (IC_{50} = 180 nM, n= 4) compared with $\alpha\beta\delta\varepsilon$- and $\alpha_3\beta_2$-nAChRs. There was no recovery after application of haditoxin. Finally, we tested the effect of haditoxin on $\alpha_4\beta_2$-nAChRs. Application of 10 μM haditoxin blocked only 70% of the current with partial reversibility **(Fig. 4G)**. The IC_{50} value of the blockade is in the micromolar range (IC_{50} = 2.6 μM, n = 3) **(Fig. 4H)**. However, further experiments will be necessary to discriminate between the different mechanisms of blockade and recovery. These results show that haditoxin had a higher potency for α_7-nAChRs than for the other nAChRs. IC_{50} values for $\alpha\beta\delta\varepsilon$- and $\alpha_3\beta_2$-nAChRs were in the same nanomolar range, whereas for $\alpha_4\beta_2$-nAChRs, it was in the micromolar range.

Haditoxin is a dimer

During the gel filtration of the crude venom we observed that haditoxin eluted earlier compared to other 3FTxs (**Fig. 2A**, most of the 3FTxs elutes in peak 3). This led us to investigate the oligomeric states of this protein. So, we carried out analytical gel filtration experiments using a Superdex G-75 column. Protein, at concentrations (0.25 to 10 μM) covering the IC_{50} in CBCM (0.27 ± 0.07μM) and RHD (1.85 ± 0.39 μM) preparations, was loaded onto the column. At all of these concentrations, the presence of a single peak corresponding to a relative molecular weight (Mr) of 16.25 kDa was observed **(Fig. 5A)**, supporting the existence of a dimeric species. To observe the effect of SDS on dimerization, we treated the protein (0.25 to 10 μM) with SDS and eluted using the same column. It eluted as a single peak with a Mr of 8.16 kDa **(Fig. 5A)** similar to the monomeric species.

The dimerization was further confirmed by Tris-Tricine SDS-PAGE analysis in the presence and absence of a cross-linker, BS^3 **(Fig. 5B)**. In the presence of BS^3, both the dimeric and monomeric species were visualized **(Fig. 5B, lane 1)** whereas only the monomeric species were observed in its absence **(Fig. 5B, lane 2)**. These results, together with MS data (showing monomeric mass, **Fig 2C**), indicate the existence of haditoxin as a homodimer in solution at pharmacologically relevant concentrations and the dimerization occurs through non-covalent interactions. Further, as haditoxin loses its β-sheeted structure and becomes random coil in the presence of SDS (as indicated by CD studies; data not shown), its overall conformation may play a critical role in the dimerization.

X-ray crystal structure of haditoxin

In order to determine the three-dimensional structure of haditoxin we used X-ray crystallographic method. Diffraction quality crystals of haditoxin were obtained with 0.1 M Tris, pH 8.5, 20% v/v ethanol (Hampton Research crystal screen 2, condition no. 44). Diffraction up to 1.55 Å was observed and the crystals belonged to the space group $P2_1$ **(Table I)**.

Structure determination and refinement

The structure of haditoxin was solved by molecular replacement method (Molrep) (50). Initially, toxin-α, isolated from *Naja nigricollis* venom was used as a search model (pdb code 1IQ9; sequence identity ~48%). The rotation and translation resulted in a correlation factor of 0.07 and R_{cryst} of 0.57. Further minimization in Refmac (51) reduced the R factor to 0.42. An excellent quality electron density map was calculated at this stage which allowed to auto-build 90% of the haditoxin model with ARP/wARP (52). Resulting model with the electron density map was examined to manually build the rest of the model using Coot program (53). After a few cycles of map fitting and refinement, we obtained an R factor of 0.194 (R_{free}=0.225) for reflections I>σI within 20-1.55 Å resolution. Throughout the refinement **(Table I)** no NCS restraint was employed. All the 65 residues (considering one subunit) are well defined in the electron density map **(Fig. 6A)** and statistics for the Ramachandran plot using PROCHECK (54) showed the presence of 88.9% of non-glycine residues in the most

favored region. The coordinates and structure factors have been deposited with the RCSB PDB (55) with the code 3HH7. The asymmetric unit consists of two monomers forming a tight dimer having an approximate dimension of 25 X 13 X 4 Å **(Fig. 6B)**. This crystallographic dimer is consistent with the gel filtration and SDS-PAGE observations **(Fig. 5)**. Both the monomers are related by a 2-fold symmetry and their superposition yielded an rmsd of 0.2 Å for 65 Cα atoms **(Fig. 7A)**. Each monomer adopts the common "three-finger" fold (11) consisting of three β-sheeted loops protruding from a central core, tightened by four highly conserved disulfide bridges (Cys3–Cys24, Cys17–Cys41, Cys45–Cys57 and Cys58–Cys63) **(Fig. 6B and C)** and are structurally similar to short-chain α-neurotoxins like toxin-α and erabutoxins **(Fig. 7B)**. Loop I forms a two-stranded β-sheet (Lys2–Tyr4 and Thr14–Ile16), whereas loops II and III form a three-stranded β-sheet (Glu34–Thr42, Phe23–Asp31 and Lys53–Cys58). The anti-parallel β-strands of the β-sheet are stabilized by mainchain–mainchain hydrogen bonding.

Dimeric interface

The dimeric interface was analysed using the PISA server (56). It is mainly formed by loop III of each subunit. Strands D, C, E, E', C' and D' form a six β-pleated sheet with an overall right-handed twist **(Fig. 6B)** in the dimer. Approximately 565 $Å^2$ (or 12% of the total) surface areas and 17 residues of each monomer contribute to the dimerization. The close contacts between the monomers are maintained by 14 hydrogen bonds (< 3.2 Å) and extensive hydrophobic interactions **(Table II)**. Six mainchain–mainchain hydrogen bonding contacts exist across the interface involving strand E of monomer A and E' of B **(Table II, Fig. 7C)**; four are observed between the mainchain amide hydrogen and carbonyl oxygen of Val55 and Cys57 from monomer A and Val55' and Cys57' from monomer B; and the remaining two exist between the carbonyl oxygen of Lys53 (and Lys53') and the amide hydrogen of Arg59 (and Arg59'). In addition, there are another eight hydrogen bonding contacts mediated through the side chains of Thr44, Cys45, Glu47, Pro50 and Arg59 **(Table II, Fig. 7C)**. Two hydrophobic clusters further stabilize the dimeric structure. The side chains of Phe23 and Leu48 from both monomers form one cluster, whereas the disulphide bridge between Cys45-Cys57 and Val55 of both monomers form the other. These observations strongly suggest the existence of haditoxin as non-covalent homodimeric species.

DISCUSSION

Nonenzymatic neurotoxins from snake venom belonging to the 3FTx family consist of closely related polypeptides with a MW range of 6500 to 8000 Daltons. Functionally, most interfere with cholinergic neurotransmission and are highly specific for different subtypes of muscarinic or nicotinic cholinergic receptors (for details see, Introduction). This underscores their immense potential as lead molecules in drug discovery and as research tools in the characterization of receptor subtypes.

Here, we have described the purification and characterization of a novel neurotoxin, Haditoxin, from the venom of *Ophiophagus hannah*. It is a non-covalent homodimer which produces potent postsynaptic neuromuscular blockade of the mammalian (IC_{50} = 1.85 ± 0.39 μM and avian muscle (IC_{50} = 0.27 ± 0.07 μM) (αβγδ) nAChRs **(Fig. 3A and 3C)**. In electrophysiological studies, it was an antagonist of muscle (αβδε) (IC_{50} = 0.55 μM) as well as neuronal α_7- (IC_{50} = 0.18 μM), $\alpha_3\beta_2$- (IC_{50} = 0.50 μM) and $\alpha_4\beta_2$- (IC_{50} = 2.60 μM) nAChRs **(Fig 4)**. Interestingly, haditoxin exhibited a novel pharmacology with combined blocking activity on muscle (αβγδ) as well as neuronal (α_7, $\alpha_3\beta_2$ and $\alpha_4\beta_2$) nAChRs but with the highest potency on α_7-nAChRs, which is recognized by neither short chain α-neurotoxins nor κ-neurotoxins.

The reversibility of this neuromuscular blockade was taxa-specific; it is partially reversible by washing in the chick neuromuscular junction, whereas it was almost irreversible in the rat neuromuscular junction. Earlier, we reported taxa-specific

neurotoxicity of denmotoxin from *Boiga dendrophila* (12) and irditoxin from *Boiga irregularis* (13). Taxa-specificity manifests the natural targeting of the venom toxins towards their prey (13;57-59). Snakes from the *Boiga* sp. mainly feeds on the non-mammalian prey like birds (12;13;60), whereas elapids including the king cobra, mainly prey on snakes and rodents, and only occasionally and opportunistically on birds (61;62). Venom compositions of snakes are known to be dependent on prey specificity, in order to ensure efficiency in their capture and killing (58). Therefore, the taxa-specific reversibility of the neuromuscular blockade produced by haditoxin is likely due to the natural species-specificity of the king cobra venom and not because of low toxicity.

Structurally important residues for haditoxin

Haditoxin contains all eight conserved cysteine residues that are essential for the three-finger folding (24;63). They form four disulfide bridges located in the core region of the molecule. In addition, this molecule possesses several other structurally invariant residues, responsible for the stability of the three-finger fold. For example, Tyr25 (numbering of the residues are according to erabutoxin-a, unless stated otherwise), the crucial residue stabilizing the antiparallel β-sheet structure (64), is conserved in a similar three dimensional orientation. Similarly, the structurally invariant Gly40, involved in the tight packing of the three dimensional fold by accommodating the bulky side chain of the Tyr25 (24) is also conserved. The two proline residues Pro44 and Pro48, potentially associated with the formation of the β-turn (24) are conserved in haditoxin as Pro46 and Pro50. The salt bridge between the N-terminal amino group and the carboxyl group of Glu58 as well as the C-terminal carboxyl group and the guanidinium group of Arg39 in erabutoxin-a (24) is maintained by the N-terminal amino group and the carboxyl group of Asp58 as well as the C-terminal carboxyl group and the guanidinium group of the Arg39 in haditoxin. Thus, the presence of these structurally invariant residues contributes to the stable three-finger fold of haditoxin.

Functionally important residues for haditoxin

Extensive structure-function relationship studies on the short-chain α-neurotoxin, erabutoxin-a (24;65;66), and long-chain α-neurotoxins, α-cobratoxin (67;68) and α-bungarotoxin (69;70), revealed the critical residues involved in the recognition of nAChRs by snake neurotoxins. The crucial residues for α-neurotoxins to bind to muscle (αβγδ) nAChRs are Lys27, Trp29, Asp31, Phe32, Arg33, and Lys47. Haditoxin possesses three of them (Trp29, Asp31 and Arg33) in homologous positions. Additionally, each type of toxin possesses specific residues that recognized muscle or neuronal nAChRs. For muscle (αβγδ) nAChRs, these are His6, Gln7, Ser8, Ser9, and Gln10 in loop I and Tyr25, Gly34, Ile36, and Glu38 in loop II of short-chain α-neurotoxins (65) and Arg36 in loop II and Phe65 in the C-terminus tail of long-chain α-neurotoxins (67). His6, Gln7 and Ser8 in the loop I and Tyr25, Gly34, Ile37 and Glu38 in the loop II are conserved in haditoxin as the muscle-subtype specific determinants of short-chain α-neurotoxins. Moreover, Arg36, muscle-subtype specific determinant of long-chain α-neurotoxins is also conserved in haditoxin. The presence of these multiple functional determinants may explain the potent neurotoxicity exhibited by haditoxin on mammalian and avian muscle (αβγδ) nAChR.

On the contrary, the specific determinants (Ala28 and Lys35; α-cobratoxin numbering) of long-chain α-neurotoxins towards the neuronal (α_7) nAChRs (71) are not conserved in haditoxin. Significantly, haditoxin also lacks the 5th disulfide bridge responsible for the cyclization of loop II which is considered to be a hallmark determinant for the ability of neurotoxins such as α-bungarotoxin and κ-bungarotoxins to interact with their specific neuronal nAChR targets (67;71-74). This is somewhat surprising given the high affinity of haditoxin for α_7- (IC_{50} = 0.18 μM), $\alpha_3\beta_2$- (IC_{50} = 0.5 μM) and $\alpha_4\beta_2$- (IC_{50} = 2.6 μM) nAChRs. Previously, candoxin, a non-conventional

3FTx (31) was found to be an exception of a 3FTx that did not have the 5th disulfide bridge in loop II (candoxin has a 5th disulfide bridge in loop I), but still retained the ability to interact with neuronal (α_7) nAChRs (75). It was suggested thus that candoxin may likely interact with neuronal α_7-nAChRs using alternate, novel points of contact. Likewise, it is plausible that haditoxin possesses unique combinations of determinants which enable its interaction with α_7-, as well as $\alpha_3\beta_2$- and $\alpha_4\beta_2$-nAChRs. A detailed structure-function analysis to decipher these novel determinants is beyond the scope of this report.

In the case of κ-neurotoxins which interact with neuronal $\alpha_3\beta_2$- and $\alpha_4\beta_2$-nAChRs with high affinity (26;27), the critical functional residue was identified as Arg34 (76). Haditoxin has Arg33 in a homologous position, which may contribute in part to high affinity interaction with $\alpha_3\beta_2$- (IC_{50} = 0.5 μM) and $\alpha_4\beta_2$- (IC_{50} = 2.6 μM) nAChRs. Mutagenesis studies on κ-bungarotoxin revealed that the replacement of Pro36 to an amino acid residue bearing a bulky, charged sidechain, like the Lys found in α-bungarotoxin, causes a 16-fold decrease in the efficacy of the toxin to block neurotransmission in the chick ciliary ganglion assay (76). Haditoxin bears an equivalent glycine residue, lacking a bulky, charged sidechain, which can explain the high affinity of this toxin towards the neuronal ($\alpha_3\beta_2$ and $\alpha_4\beta_2$) nAChRs.

Comparison of haditoxin with other dimeric 3FTxs

Few known examples of dimeric three-finger neurotoxins derived from snake venoms exist (13;37;72). Amongst them, the most well studied and characterized are the κ-neurotoxins, known to be composed of two identical monomers held together by non-covalent interactions (77;78). The observed dimeric form of haditoxin, with the characteristic six β-pleated sheets, is similar to that formed by κ-bungarotoxin (77). Superposition of both molecules yielded an rmsd of 1.95 Å for 104 Cα atoms **(Fig. 8A)**. The major deviations are located in the loops between the antiparallel β-strands. However, each monomer in κ-bungarotoxin is structurally homologous to long-chain α-neurotoxins unlike haditoxin which resembles short-chain α-neurotoxins **(Fig. 7C)**. The dimeric interface for both is maintained by six mainchain-mainchain hydrogen bonds (77). In addition, haditoxin has eight sidechain hydrogen bonding contacts between the monomers, whereas only three similar contacts were observed in κ-bungarotoxin **(Fig. 7A)** (77), suggesting that haditoxin forms tighter dimers than κ-bungarotoxin. The side chain interactions in κ-bungarotoxin are maintained by Phe49, Leu57, and Ile20, which are strictly conserved in all κ-neurotoxins (77;79). Mutagenesis studies have proven that replacing Phe49 or Ile20 with alanines renders a toxin with an apparent lack of ability to fold into the native structure, even as a monomer (79). The same result has been observed with deletion studies (deletion of Arg54) with an aim to generate a 65 residue long protein, as found in the α-neurotoxins, from the 66 residue long κ-bungarotoxin (79). Whereas haditoxin being a 65 residue long protein lacks both Phe49 and Ile20 but still retains the intact dimeric structure. The electrostatic surface potential for both the molecules were apparently similar **(Fig. 8B)** except for the tip of loop II which revealed a strong positive patch for haditoxin compared to κ-bungarotoxin (77).

Functionally κ-neurotoxins interact with the neuronal ($\alpha_3\beta_2$ and $\alpha_4\beta_2$) nAChRs with high affinity (26;27), whereas haditoxin interacts with both muscle ($\alpha\beta\gamma\delta$) and a variety of neuronal (α_7, $\alpha_3\beta_2$ and $\alpha_4\beta_2$) nAChRs. The crystal structure of the κ-bungarotoxin dimer showed that the guanidinium groups of the essential arginine residues, situated at the tip of the loop II, maintains nearly identical distance (44 Å) (77) as like the acetylcholine binding sites in the pentameric receptor (30-50 Å) (80;81). The κ-bungarotoxin dimer may interact with both the acetylcholine binding sites on a single neuronal receptor and physically block ion flow by spanning the channel (77;79). But this mode of interaction does not explain the inability of the κ-neurotoxins to block the muscle nAChRs.

Haditoxin maintains a distance of ~52 Å between the guanidinium groups of the critical arginine residues present in the turn region of the second loop which is almost similar to the acetylcholine binding sites in the pentameric receptor mentioned above. But unlike the κ-neurotoxins, haditoxin interacts with both muscle and neuronal nAChRs. This supports the fact that the dimeric toxins may have a unique mode of interaction with the nAChRs which demands further investigation.

More recently, other heterodimeric 3FTxs from elapid venoms have been reported, including covalently (disulfide) linked homodimers of a long-chain α-neurotoxin (α-cobratoxin) and heterodimers of α-cobratoxin in combination with a variety of three-finger cytotoxins (72). Unlike haditoxin, all of these dimers are formed by covalent bonding (disulfide linkage) of the monomeric units. Functionally, the α-cobratoxin-cytotoxin heterodimers were able to block neuronal (α_7) nAChRs whereas the α-cobratoxin homodimer exhibited blockade of both neuronal α_7- and $\alpha_3\beta_2$-nAChRs, unlike monomeric α-cobratoxin which interacts with muscle ($\alpha\beta\gamma\delta$) and neuronal (α_7) nAChRs (72).

Our laboratory has also reported on a colubrid venom derived covalently linked heterodimeric 3FTx, irditoxin (13), which was found to target muscle ($\alpha\beta\gamma\delta$) nAChRs, in sharp contrast to the reported function of elapid dimeric toxins (72). Another distinguishing feature was that the subunits of irditoxin structurally resemble nonconventional 3FTxs (13). Haditoxin, is both structurally and functionally distinct from the α-cobratoxin hetero/homodimers as well as irditoxin. Structurally, haditoxin is a non-covalently-linked homodimer of the short-chain α-neurotoxin type and functionally, it has a broad pharmacological profile with high affinity and selectivity for muscle ($\alpha\beta\gamma\delta$) and neuronal (α_7, $\alpha_4\beta_2$ and $\alpha_3\beta_2$) nAChRs. Haditoxin exhibits a unique structural and functional profile and is the first reported dimeric three-finger toxin (3FTx) interacting with the muscle ($\alpha\beta\gamma\delta$) nAChR as well as the first short-chain type of α-neurotoxin to interact with neuronal α_7-nAChR with nanomolar affinity.

Acknowledgements

This work was supported by research grant from the Biomedical Research Council (BMRC), Agency for Science and Technology, Singapore, to Professor R. M. Kini (BMRC grant no. R154-000-172-316). A/P J. Sivaraman acknowledges the AcRF funding support (grant number R154000438112) from NUS, Singapore.

LEGENDS FOR THE FIGURES

Figure 1: Multiple sequence alignment of novel proteins. Sequence allignment of haditoxin with the (A) most homologous sequences, (B) muscarinic toxin homologs and (C) short-chain α-neurotoxins. Toxin names, species, and accession numbers are shown. Conserved residues in all sequences are highlighted in black. Disulfide bridges and loop regions are also shown. At the end of each sequences, the number of amino acids are stated. The homology (sequence identity and similarity) of each protein is compared with haditoxin and shown at the end of each sequence.

Figure 2: Purification of haditoxin from the venom of *O. hannah*. (A) Gel filtration chromatogram of crude venom. Crude venom (100 mg/ml) was fractionated using a Superdex 30 Hiload (16/60) column. Column was pre-equilibrated with 50 mM Tris-HCl buffer (pH 7.4). Proteins were eluted at a flow rate of 1 ml/min using the same buffer. A black bar at peak 2 indicates the fractions containing haditoxin. (B) RP-HPLC profile of the gel filtration fractions containing haditoxin. Jupiter C18 (5 µ, 300 Å, 4.5 x 250 mm) analytical column was equilibrated with 0.1% (v/v) TFA. Protein of interest was eluted from the column with a flow rate of 1 ml/min with a gradient of 23-49% buffer B (80% acetonitrile in 0.1% TFA). The dotted line (- - -) indicates the gradient of the buffer B. Downward arrow at peak 2a indicates fractions containing haditoxin. (C) ESI-MS profile of the RP-HPLC fraction containing haditoxin. The spectrum shows a series of multiply charged ions, corresponding to a single, homogenous peptide with a molecular weight of 7535.88 Da. *Inset*- reconstructed mass spectrum of haditoxin, CPS = counts/s; amu = atomic mass units. (D) Far-UV CD spectrum of haditoxin. The protein was dissolved in MilliQ water (0.5 mg/ml), and the CD spectra were recorded using a 0.1 cm path-length cuvette and (E) Electropherogram of haditoxin. The sample was injected using pressure mode 5 p.s.i./s, and electrophoresis runs were carried out using a coated capillary (17 cm x 25 µm) at 18 kV, with 0.1 M phosphate buffer (pH 2.5) at 20 °C for 7 min.

Figure 3: Pharmacological profile of haditoxin. A segment of tracing showing the effect of haditoxin (1.5 µM) on (A) Chick biventer cervicis muscle preparations (CBCM), (B) reversibility of CBCM preparation, (C) rat hemidiaphragm muscle (RHD) preparations and (D) reversibility of RHD preparation. Contractions were produced by exogenous acetylcholine (ACh; 300 µM), carbachol (CCh; 10 µM), and KCl (30 mM). The black bar indicates the electrical field stimulation (EFS). The point of washing out the toxin with krebs solution in reversibility studies is indicated by the abbreviation 'W'. (E) Dose-response curve of haditoxin and α-bungarotoxin on CBCM and RHD. The block is calculated as a percentage of the control twitch responses of the muscle to supramaximal nerve stimulation. Each data point is the mean ± S.E. of at least three experiments. (F) Comparitive reversibility profile of α-bungarotoxin, haditoxin and candoxin.

Figure 4: Effect of haditoxin on human nACHRs expressed in Xenopus oocytes. Inhibition of ACh-induced currents in (A) αβδε- (neuromuscular junction), (C) α_7-, (E) $\alpha_4\beta_2$- and (G) $\alpha_3\beta_2$-nAChRs. NMJ currents were activated by 10 µM ACh, whereas 200 µM was used to activate α_7-, $\alpha_4\beta_2$- and $\alpha_3\beta_2$-nAChRs. First three traces are controls, followed by 2 minutes exposure to several haditoxin concentrations ranging from 10 nM to 10 µM. Each experiment was terminated by 8 minutes wash out. Little or no recovery was observed for αβδε- and α_7-nAChRs, whereas partial to full recovery was observed for $\alpha_4\beta_2$- and $\alpha_3\beta_2$-nAChRs. Inhibition curves of the fitted data, IC_{50} and Hill coefficient (nH) for (B) αβδε-nAChRs were 0.55 µM and 0.7, (D) α_7-nAChRs were 0.18 µM and 0.8, (F) for $\alpha_3\beta_2$-nAChRs were 0.5 µM and 1.1 and (H) for $\alpha_4\beta_2$-nAChRs were 2.6 µM and 0.7.

Figure 5: Dimerization of haditoxin. (A) Gel filtration profile of haditoxin with (gray) and without (black) SDS. 1 μM of haditoxin was loaded onto a Superdex 75 column (1 cm x 30 cm) equilibrated with 50 mM Tris-HCl buffer (pH 7.4). The protein was eluted out with the 50 mM Tris-HCl buffer (pH 7.4) or 50 mM Tris-HCl buffer (pH 7.4) containing 0.6% SDS at flow rate of 0.6 ml/min and (B) Tris-tricine SDS-PAGE analysis of haditoxin with (lane 1) and without (lane 2) cross linker (BS^3). M is the marker lane. Concentration of BS^3 is 5 mM.

Figure 6: Overall structure of haditoxin. (A) Stereo view of a portion of the final 2Fo-Fc map of haditoxin. The map was contoured at a level of 1.0σ, (B) Monomer A and B is shown in blue and red respectively. Disulfide bonds are shown in yellow. N- and C-terminals, β-strands and loops I, II and III are labeled and (C) Structure based alignment of three-finger toxins. Color coding of conserved residues are donated by boxed red text and invariant residues by red highlight. Accession numbers are shown on the left Secondary structural elements of haditoxin are shown on top. Numbering is shown for haditoxin only. Sequence alignment was done by Strap (82) and displayed with ESPript (83).

Figure 7: Structural details of haditoxin. (A) Superimposition of both the subunits of haditoxin. Subunit A and B is shown in blue and red respectively, (B) Superimposition subunit A of haditoxin with short-chain α-neurotoxins. Subunit A is shown in blue, erabutoxin-a in magenta, erabutoxin-b in cyan and toxin-α in green and (C) Stereo diagram of comparison of dimer interface of haditoxin (top) and κ-bungarotoxin (bottom). The residues to form the hydrogen bonds are labeled. The mainchain-mainchain hydrogen bonds are shown in red. The other hydrogen bonds are shown in yellow.

Figure 8: Haditoxin vs κ-bungarotoxin. (A) Superimposition of haditoxin with κ-bungarotoxin. Haditoxin and κ-bungarotoxin is shown in red and yellow respectively and (B) Electrostatic surface of haditoxin (top) and κ-bungarotoxin (bottom). The orientation is the same as the Figure 6B. The location of Arg33 and Glu34 of haditoxin and Arg34 of κ-bungarotoxin are indicated.

Reference List

1. Harvey AL (1991) *Snake Toxins*, Pergamon Press , New York
2. Lewis, R. J. and Garcia, M. L. (2003) *Nat.Rev.Drug Discov.* **2,** 790-802
3. Harvey, A. L. (2002) *Trends Pharmacol.Sci.* **23,** 201-203
4. Langley, J. N. (1907) *J.Physiol* **36,** 347-384
5. Katz , B. and Thesleff , S. (1957) *J.Physiol* **138,** 63-80
6. Grutter, T. and Changeux, J. P. (2001) *Trends Biochem.Sci.* **26,** 459-463
7. Changeux, J. P. (1990) *Trends Pharmacol.Sci.* **11,** 485-492
8. Taylor, P., Molles, B., Malany, S., and Osaka, H. (2002) Toxins as probes for structure and specificity of synaptic target proteins. In Menez A, editor. *Perspectives in molecular toxinology*, John Wiley & Sons, Chichester, England
9. Changeux, J. P., Kasai, M., and Lee, C. Y. (1970) *Proc.Natl.Acad.Sci.U.S.A* **67,** 1241-1247
10. Colquhoun, L. M. and Patrick, J. W. (1997) *Adv.Pharmacol.* **39,** 191-220
11. Kini, R. M. (2002) *Clin.Exp.Pharmacol.Physiol* **29,** 815-822
12. Pawlak, J., Mackessy, S. P., Fry, B. G., Bhatia, M., Mourier, G., Fruchart-Gaillard, C., Servent, D., Menez, R., Stura, E., Menez, A., and Kini, R. M. (2006) *J.Biol.Chem.* **281,** 29030-29041
13. Pawlak, J., Mackessy, S. P., Sixberry, N. M., Stura, E. A., le Du, M. H., Menez, R., Foo, C. S., Menez, A., Nirthanan, S., and Kini, R. M. (2009) *FASEB J.* **23,** 534-545
14. Pahari, S., Mackessy, S. P., and Kini, R. M. (2007) *BMC.Mol.Biol.* **8,** 115
15. Jiang, M., Haggblad, J., and Heilbronn, E. (1987) *Toxicon* **25,** 1019-1022
16. Tsetlin, V. (1999) *Eur.J.Biochem.* **264,** 281-286
17. Kumar, T. K., Jayaraman, G., Lee, C. S., Arunkumar, A. I., Sivaraman, T., Samuel, D., and Yu, C. (1997) *J.Biomol.Struct.Dyn.* **15,** 431-463
18. de Weille, J. R., Schweitz, H., Maes, P., Tartar, A., and Lazdunski, M. (1991) *Proc.Natl.Acad.Sci.U.S.A* **88,** 2437-2440

19. McDowell, R. S., Dennis, M. S., Louie, A., Shuster, M., Mulkerrin, M. G., and Lazarus, R. A. (1992) *Biochemistry* **31,** 4766-4772

20. Rajagopalan, N., Pung, Y. F., Zhu, Y. Z., Wong, P. T., Kumar, P. P., and Kini, R. M. (2007) *FASEB J.* **21,** 3685-3695

21. Ricciardi, A., le Du, M. H., Khayati, M., Dajas, F., Boulain, J. C., Menez, A., and Ducancel, F. (2000) *J.Biol.Chem.* **275,** 18302-18310

22. Ohno, M., Menez, R., Ogawa, T., Danse, J. M., Shimohigashi, Y., Fromen, C., Ducancel, F., Zinn-Justin, S., le Du, M. H., Boulain, J. C., Tamiya, T., and Menez, A. (1998) *Prog.Nucleic Acid Res.Mol.Biol.* **59,** 307-364

23. Nirthanan, S. and Gwee, M. C. (2004) *J.Pharmacol.Sci.* **94,** 1-17

24. Endo, T. and Tamiya, N. (1991) Structure-function relationships of postsynaptic neurotoxins from snake venoms. In Harvey AL, editor. *Snake Toxins*, Pergamon Press, New York

25. Servent, D., Antil-Delbeke, S., Gaillard, C., Corringer, P. J., Changeux, J. P., and Menez, A. (2000) *Eur.J.Pharmacol.* **393,** 197-204

26. Grant, G. A. and Chiappinelli, V. A. (1985) *Biochemistry* **24,** 1532-1537

27. Wolf, K. M., Ciarleglio, A., and Chiappinelli, V. A. (1988) *Brain Res.* **439,** 249-258

28. Servent, D. and Fruchart-Gaillard, C. (2009) *J.Neurochem.* **109,** 1193-1202

29. Harvey, A. L., Kornisiuk, E., Bradley, K. N., Cervenansky, C., Duran, R., Adrover, M., Sanchez, G., and Jerusalinsky, D. (2002) *Neurochem.Res.* **27,** 1543-1554

30. Olianas, M. C., Ingianni, A., Maullu, C., Adem, A., Karlsson, E., and Onali, P. (1999) *J.Pharmacol.Exp.Ther.* **288,** 164-170

31. Nirthanan, S., Charpantier, E., Gopalakrishnakone, P., Gwee, M. C., Khoo, H. E., Cheah, L. S., Bertrand, D., and Kini, R. M. (2002) *J.Biol.Chem.* **277,** 17811-17820

32. Lumsden, N. G., Fry, B. G., Ventura, S., Kini, R. M., and Hodgson, W. C. (2005) *Toxicon* **45,** 329-334

33. Starkov, V. G., Poliak, I., Vul'fius, E. A., Kriukova, E. V., Tsetlin, V. I., and Utkin, I. (2009) *Bioorg.Khim.* **35,** 15-24

34. Kuruppu, S., Reeve, S., Smith, A. I., and Hodgson, W. C. (2005) *Biochem.Pharmacol.* **70,** 794-800

35. Tan, L. C., Kuruppu, S., Smith, A. I., Reeve, S., and Hodgson, W. C. (2006) *Neuropharmacology* **51,** 782-788

36. Aird, S. D., Womble, G. C., Yates, J. R., III, and Griffin, P. R. (1999) *Toxicon* **37,** 609-625

37. Chiappinelli, V. A. and Lee, J. C. (1985) *J.Biol.Chem.* **260,** 6182-6186

38. Chiappinelli, V. A. and Wolf, K. M. (1989) *Biochemistry* **28,** 8543-8547

39. Ginsborg , B. L. and Warriner , J. (1960) *Br.J.Pharmacol.Chemother.* **15,** 410-411

40. Bulbring, E. (1946) *Br.J.Pharmacol.* **120,** 3-26

41. Hogg, R. C., Bandelier, F., Benoit, A., Dosch, R., and Bertrand, D. (2008) *J.Neurosci.Methods* **169,** 65-75

42. Staros, J. V. (1982) *Biochemistry* **21,** 3950-3955

43. Otwinowski, Z. and Minor, W. (1997) Processing of X-ray Diffraction Data Collected in Oscillation Mode. In Carter, C. W. and Sweet, J. R. M., editors. *Methods in enzymology*, Academic Press , New York

44. Pung, Y. F., Wong, P. T., Kumar, P. P., Hodgson, W. C., and Kini, R. M. (2005) *J.Biol.Chem.* **280,** 13137-13147

45. Coulson, F. R., Jacoby, D. B., and Fryer, A. D. (2004) *J.Pharmacol.Exp.Ther.* **308,** 760-766

46. Weiser, M., Mutschler, E., and Lambrecht, G. (1997) *Naunyn Schmiedebergs Arch.Pharmacol.* **356,** 671-677

47. Warrell, D. A., Looareesuwan, S., White, N. J., Theakston, R. D., Warrell, M. J., Kosakarn, W., and Reid, H. A. (1983) *Br.Med.J.(Clin.Res.Ed)* **286,** 678-680

48. Laothong, C. and Sitprija, V. (2001) *Toxicon* **39,** 1353-1357

49. Palma, E., Bertrand, S., Binzoni, T., and Bertrand, D. (1996) *J.Physiol* **491 (Pt 1),** 151-161

50. Vagin, A. and Teplyakov, A. (1997) *Journal of Applied crystallography* **30,** 1022-1025

51. Vagin, A. A., Steiner, R. A., Lebedev, A. A., Potterton, L., McNicholas, S., Long, F., and Murshudov, G. N. (2004) *Acta Crystallogr.D.Biol.Crystallogr.* **60,** 2184-2195

52. Perrakis, A., Morris, R., and Lamzin, V. S. (1999) *Nat.Struct.Biol.* **6,** 458-463

53. Emsley, P. and Cowtan, K. (2004) *Acta Crystallogr.D.Biol.Crystallogr.* **60,** 2126-2132

54. Laskowski, R. A., MacArthur, M. W., Moss, D. S., and Thornton, J. M. (1993) *Journal of Applied crystallography* **26,** 283-291

55. Berman, H. M., Westbrook, J., Feng, Z., Gilliland, G., Bhat, T. N., Weissig, H., Shindyalov, I. N., and Bourne, P. E. (2000) *Nucleic Acids Res.* **28,** 235-242

56. Krissinel, E. and Henrick, K. (2007) *J.Mol.Biol.* **372,** 774-797

57. Barlow, A., Pook, C. E., Harrison, R. A., and Wuster, W. (2009) *Proc.Biol.Sci.*

58. Daltry, J. C., Wuster, W., and Thorpe, R. S. (1996) *Nature* **379,** 537-540

59. Pahari, S., Bickford, D., Fry, B. G., and Kini, R. M. (2007) *BMC.Evol.Biol.* **7,** 175

60. Mackessy, S. P., Sixberry, N. M., Heyborne, W. H., and Fritts, T. (2006) *Toxicon* **47,** 537-548

61. Mehrtens, J. (1987) *Living Snakes of the World*, Sterling, New York

62. Coborn, J. (1991) *The Atlas of Snakes of the World*, TFH Publications, New Jersey

63. Menez, A., Bouet, F., Guschlbauer, W., and Fromageot, P. (1980) *Biochemistry* **19,** 4166-4172

64. Torres, A. M., Kini, R. M., Selvanayagam, N., and Kuchel, P. W. (2001) *Biochem.J.* **360,** 539-548

65. Teixeira-Clerc, F., Menez, A., and Kessler, P. (2002) *J.Biol.Chem.* **277,** 25741-25747

66. Tremeau, O., Lemaire, C., Drevet, P., Pinkasfeld, S., Ducancel, F., Boulain, J. C., and Menez, A. (1995) *J.Biol.Chem.* **270,** 9362-9369

67. Bourne, Y., Talley, T. T., Hansen, S. B., Taylor, P., and Marchot, P. (2005) *EMBO J.* **24,** 1512-1522

68. Antil, S., Servent, D., and Menez, A. (1999) *J.Biol.Chem.* **274,** 34851-34858

69. Fruchart-Gaillard, C., Gilquin, B., Antil-Delbeke, S., Le Novere, N., Tamiya, T., Corringer, P. J., Changeux, J. P., Menez, A., and Servent, D. (2002) *Proc.Natl.Acad.Sci.U.S.A* **99,** 3216-3221

70. Dellisanti, C. D., Yao, Y., Stroud, J. C., Wang, Z. Z., and Chen, L. (2007) *Nat.Neurosci.* **10,** 953-962

71. Antil-Delbeke, S., Gaillard, C., Tamiya, T., Corringer, P. J., Changeux, J. P., Servent, D., and Menez, A. (2000) *J.Biol.Chem.* **275,** 29594-29601

72. Osipov, A. V., Kasheverov, I. E., Makarova, Y. V., Starkov, V. G., Vorontsova, O. V., Ziganshin, R. K., Andreeva, T. V., Serebryakova, M. V., Benoit, A., Hogg, R. C., Bertrand, D., Tsetlin, V. I., and Utkin, Y. N. (2008) *J.Biol.Chem.* **283,** 14571-14580

73. Grant, G. A., Luetje, C. W., Summers, R., and Xu, X. L. (1998) *Biochemistry* **37,** 12166-12171

74. Servent, D., Mourier, G., Antil, S., and Menez, A. (1998) *Toxicol.Lett.* **102-103,** 199-203

75. Nirthanan, S., Charpantier, E., Gopalakrishnakone, P., Gwee, M. C., Khoo, H. E., Cheah, L. S., Kini, R. M., and Bertrand, D. (2003) *Br.J.Pharmacol.* **139,** 832-844

76. Fiordalisi, J. J., al Rabiee, R., Chiappinelli, V. A., and Grant, G. A. (1994) *Biochemistry* **33,** 3872-3877

77. Dewan, J. C., Grant, G. A., and Sacchettini, J. C. (1994) *Biochemistry* **33,** 13147-13154

78. Oswald, R. E., Sutcliffe, M. J., Bamberger, M., Loring, R. H., Braswell, E., and Dobson, C. M. (1991) *Biochemistry* **30,** 4901-4909

79. Grant, G. A., al Rabiee, R., Xu, X. L., and Zhang, Y. (1997) *Biochemistry* **36,** 3353-3358

80. Herz, J. M., Johnson, D. A., and Taylor, P. (1989) *J.Biol.Chem.* **264,** 12439-12448

81. Unwin, N. (1993) *J.Mol.Biol.* **229,** 1101-1124

82. Gille, C. and Frommel, C. (2001) *Bioinformatics.* **17,** 377-378

83. Gouet, P., Courcelle, E., Stuart, D. I., and Metoz, F. (1999) *Bioinformatics.* **15,** 305-308

Table I. X-ray data collection and refinement statistics

Data collection	
Cell parameters (Å)	a=37.27,b=41.29,c=40.98, β=106.4°
Space group	$P2_1$
Molecules /AU	2
Resolution range (Å)	50-1.55
Wavelength (Å)	1.5418
Observed reflections	82388
Unique reflections	17366
Completeness (%)	99.1(92.9)
Rsym (%)[a]	0.093
$I/\sigma(I)$	40.2(6.0)
Refinement and quality	
Resolution range (Å)	20-1.55
R_{work} (%) [b]	19.4
R_{free} (%)[c]	22.5
rmsd bond lengths (Å)	0.009
rmsd bond angles(deg)	1.274
Average B-factors (Å ^{2})	15.1
Number of protein atoms	130
Number of waters	117
Ramachandran plot (%)	
Most favored regions	88.9
Additional allowed regions	9.3
Generously allowed regions	1.9
Disallowed regions	0

[a] $R_{sym}=\sum|I_i-\langle I\rangle|/\sum|I|$, where I_i is the intensity of the *i*th measurement, and $\langle I\rangle$ is the mean intensity for that reflection.

[b] $R_{work}=\sum|F_{obs}-F_{calc}|/\sum|F_{obs}|$, where F_{calc} and F_{obs} are the calculated and observed structure factor amplitudes, respectively.

[c] R_{free}=as for R_{work}, but for 10 % of the total reflections chosen at random and omitted from refinement.

Table II Hydrogen bonds in the dimeric interface of the haditoxin

		Monomer A	Monomer B	Distance [Å]
Main-Chain	1	CYS 57[O]	VAL 55[N]	2.93
	2	VAL 55[O]	CYS 57[N]	2.85
	3	CYS 57[N]	VAL 55[O]	2.86
	4	VAL 55[N]	CYS 57[O]	2.90
	5	LYS 53[O]	ARG 59[N]	3.10
	6	ARG 59[N]	LYS 53[O]	3.40
Side-Chain	7	GLU 47[OE1]	THR 44[OG1]	2.63
	8	GLU 47[OE2]	CYS 45[N]	2.76
	9	PRO 50[O]	ARG 59[NE]	3.39
	10	THR 49[O]	ARG 59[NH2]	3.37
	11	THR 44[OG1]	GLU 47[OE1]	2.68
	12	CYS 45[N]	GLU 47[OE2]	2.81
	13	ARG 59[NH2]	THR 49[O]	2.66
	14	ARG 59[NE]	GLY 52[O]	2.76

Figure 1

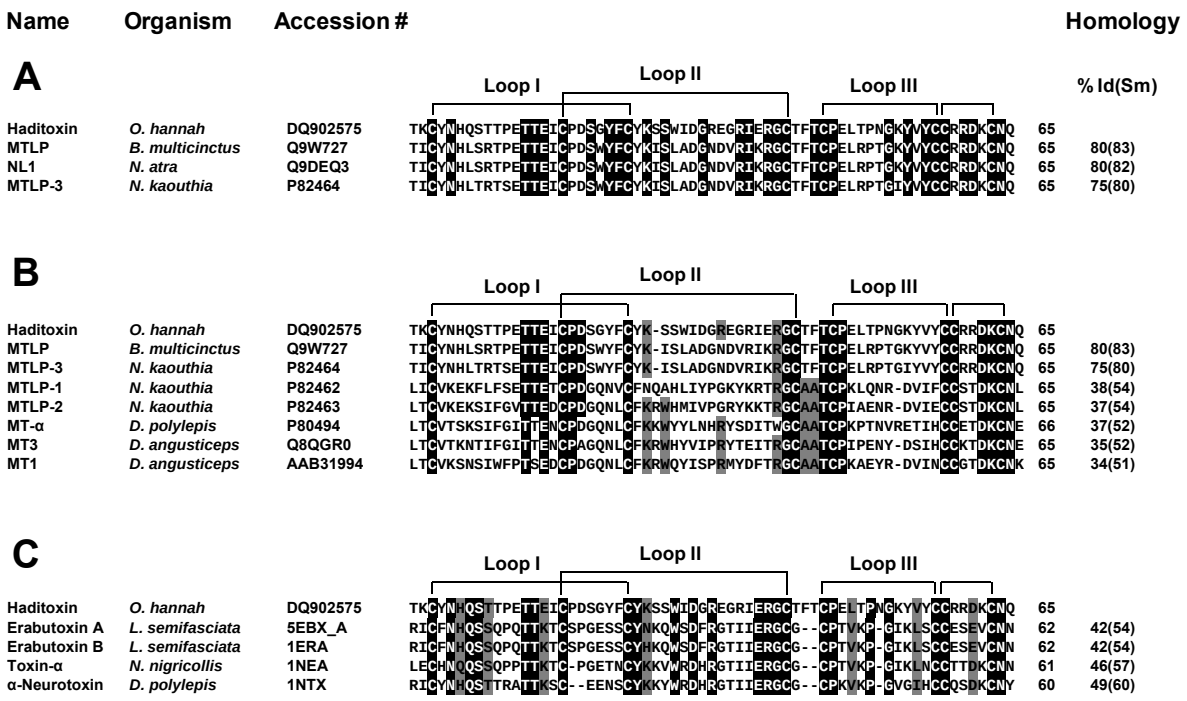

Figure 2

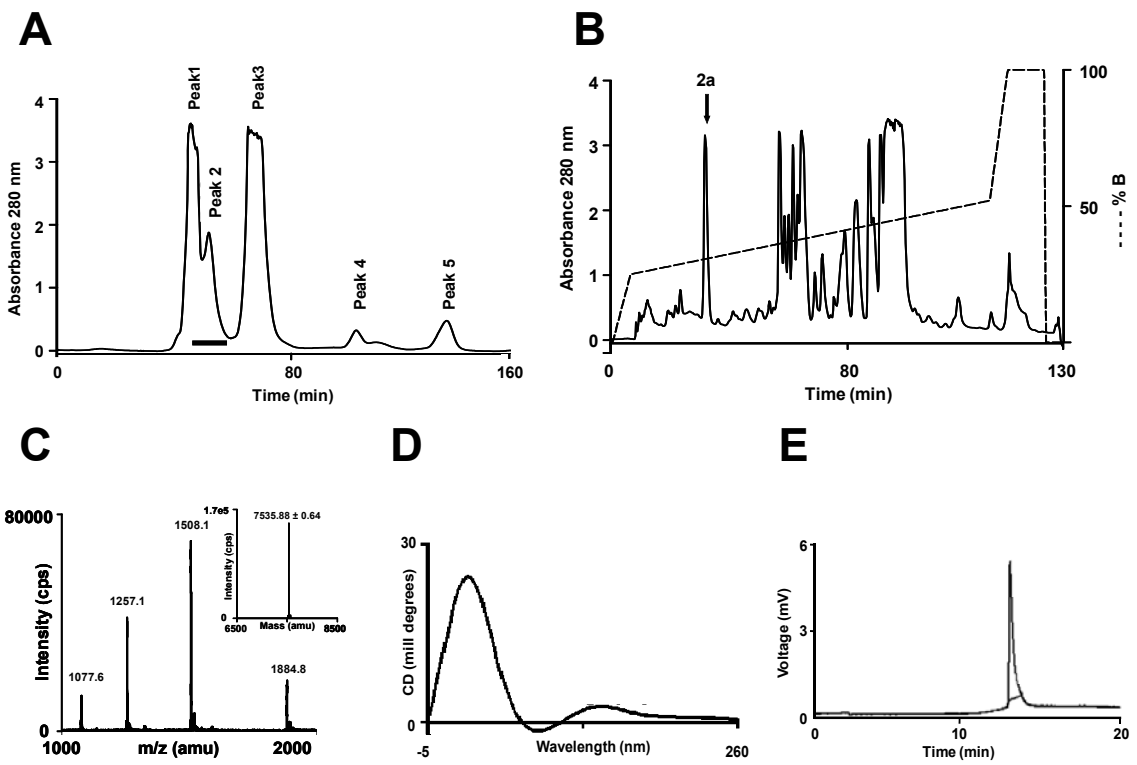

Figure 3

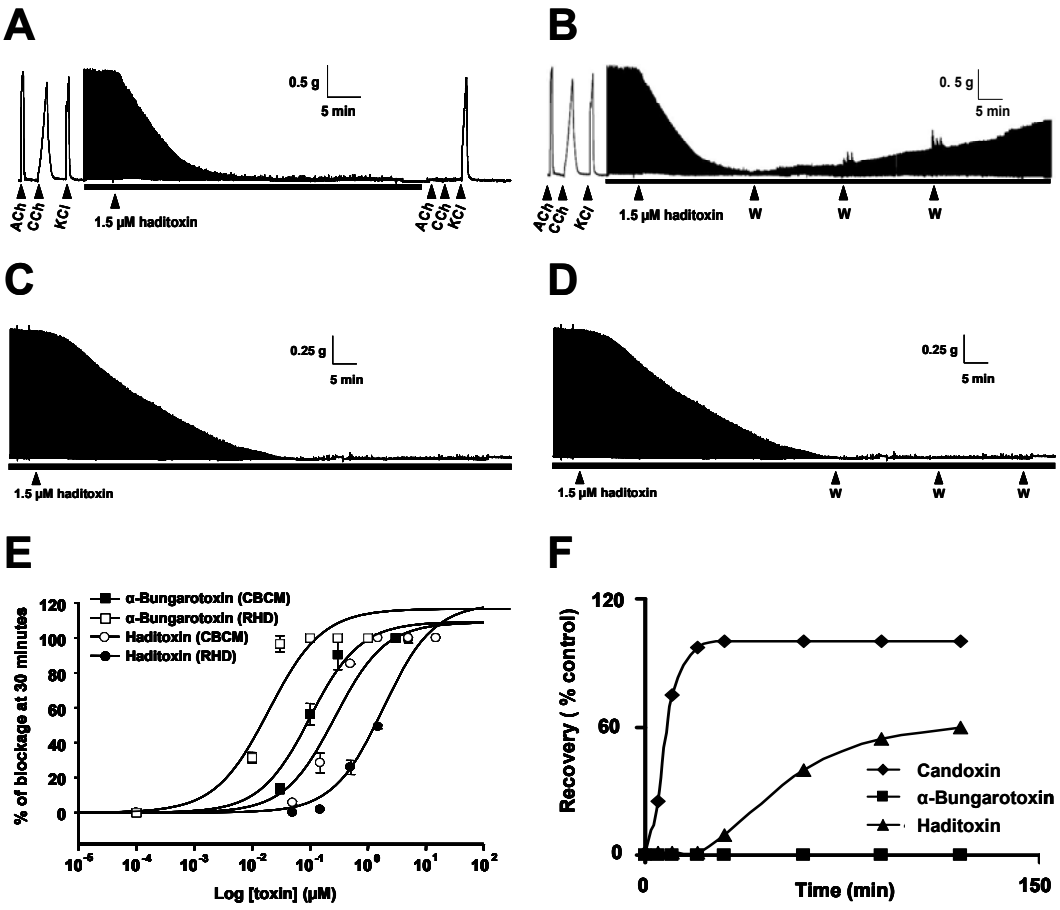

Figure 4

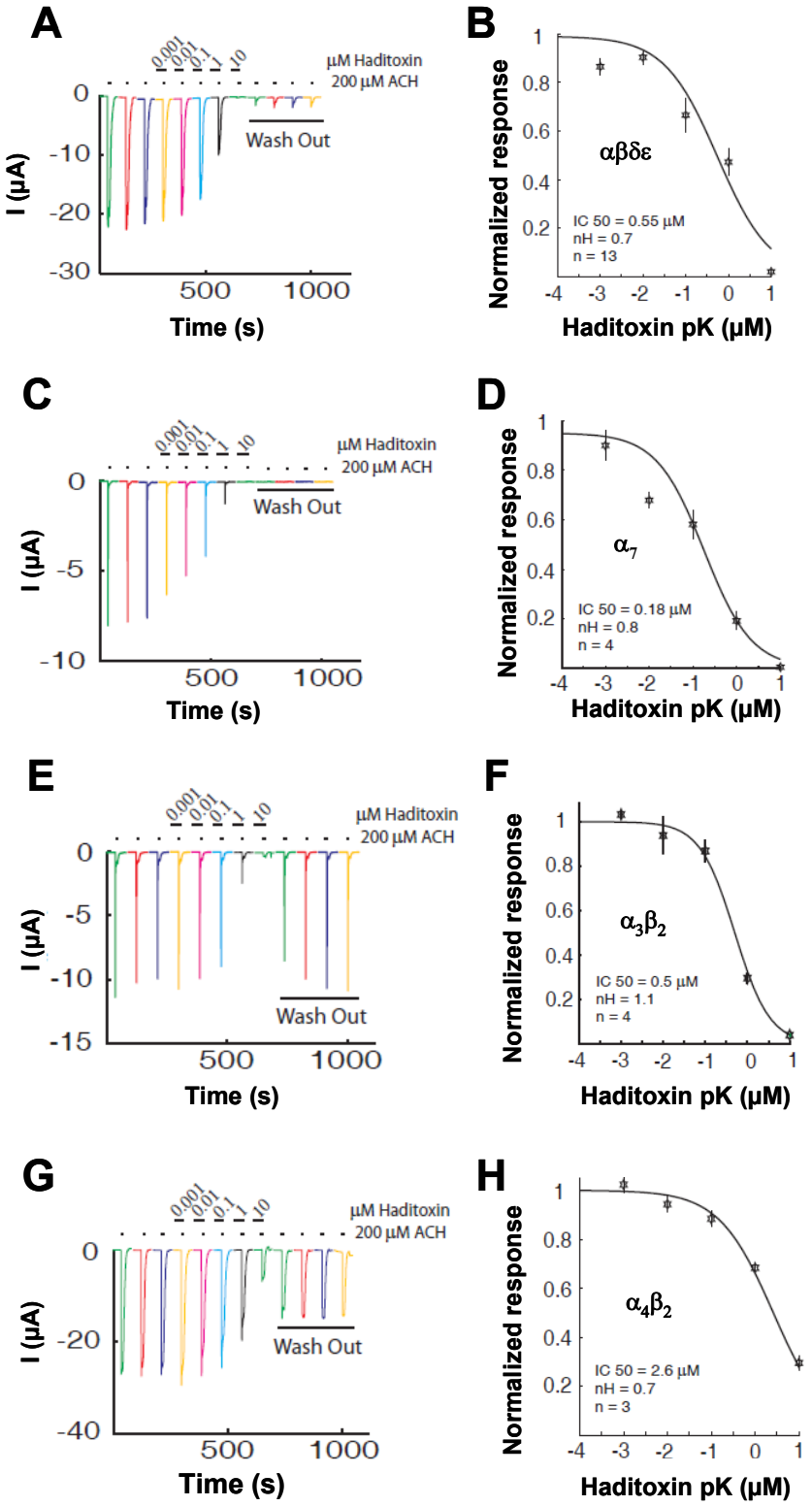

Figure 5

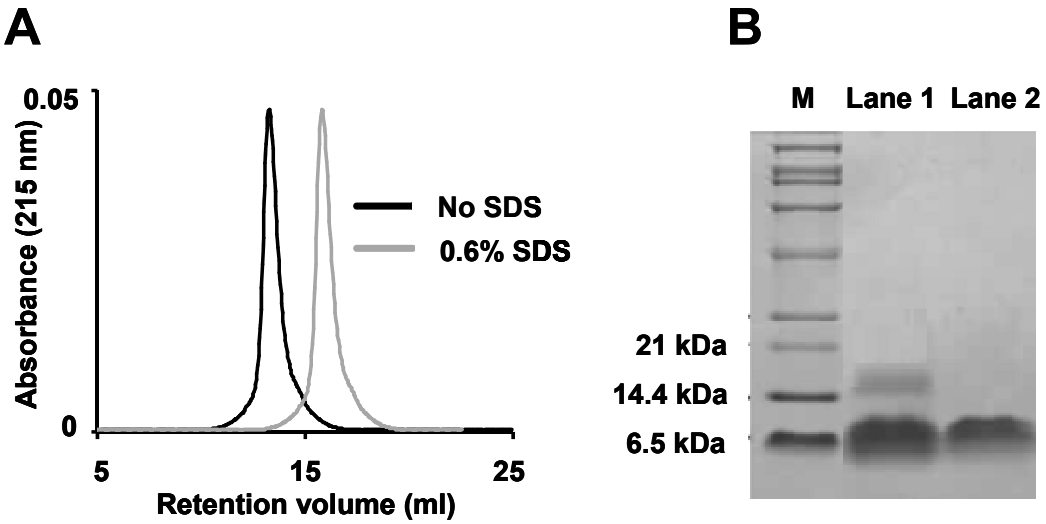

Figure 6

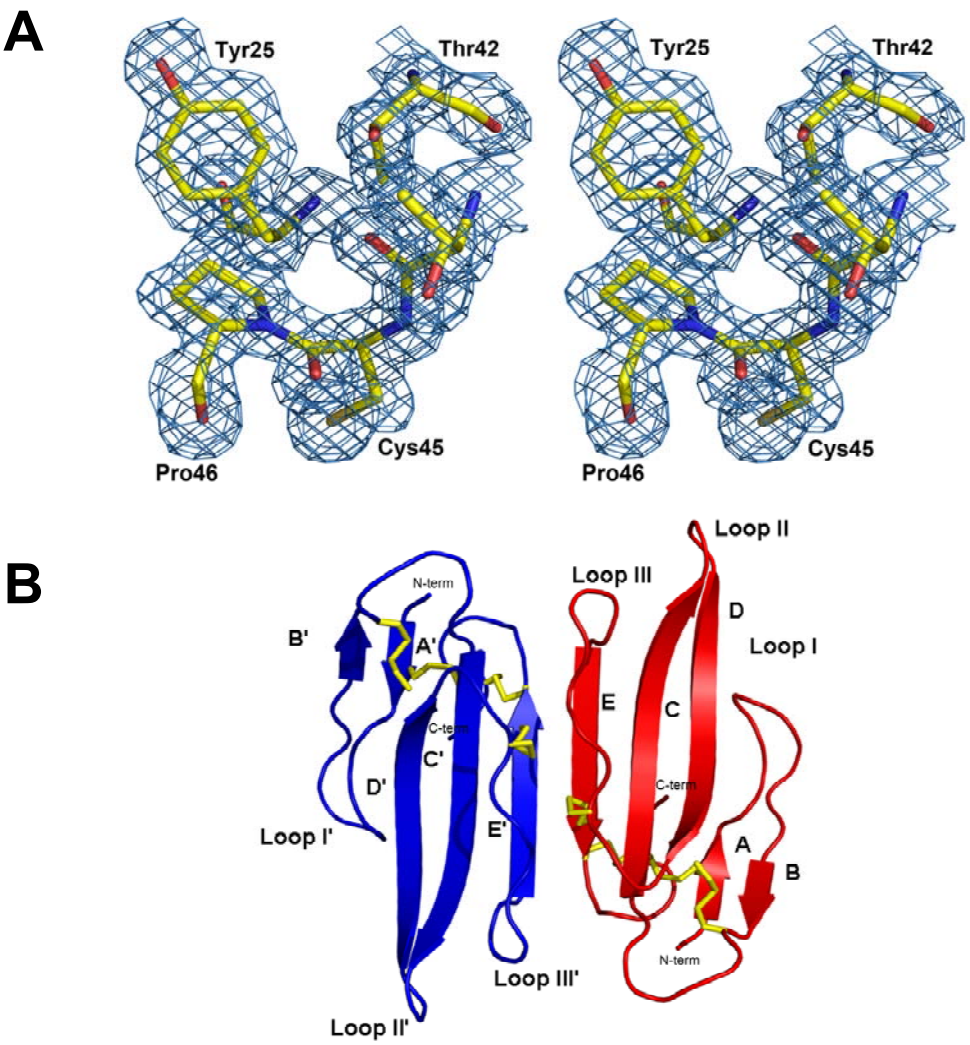

Figure 7

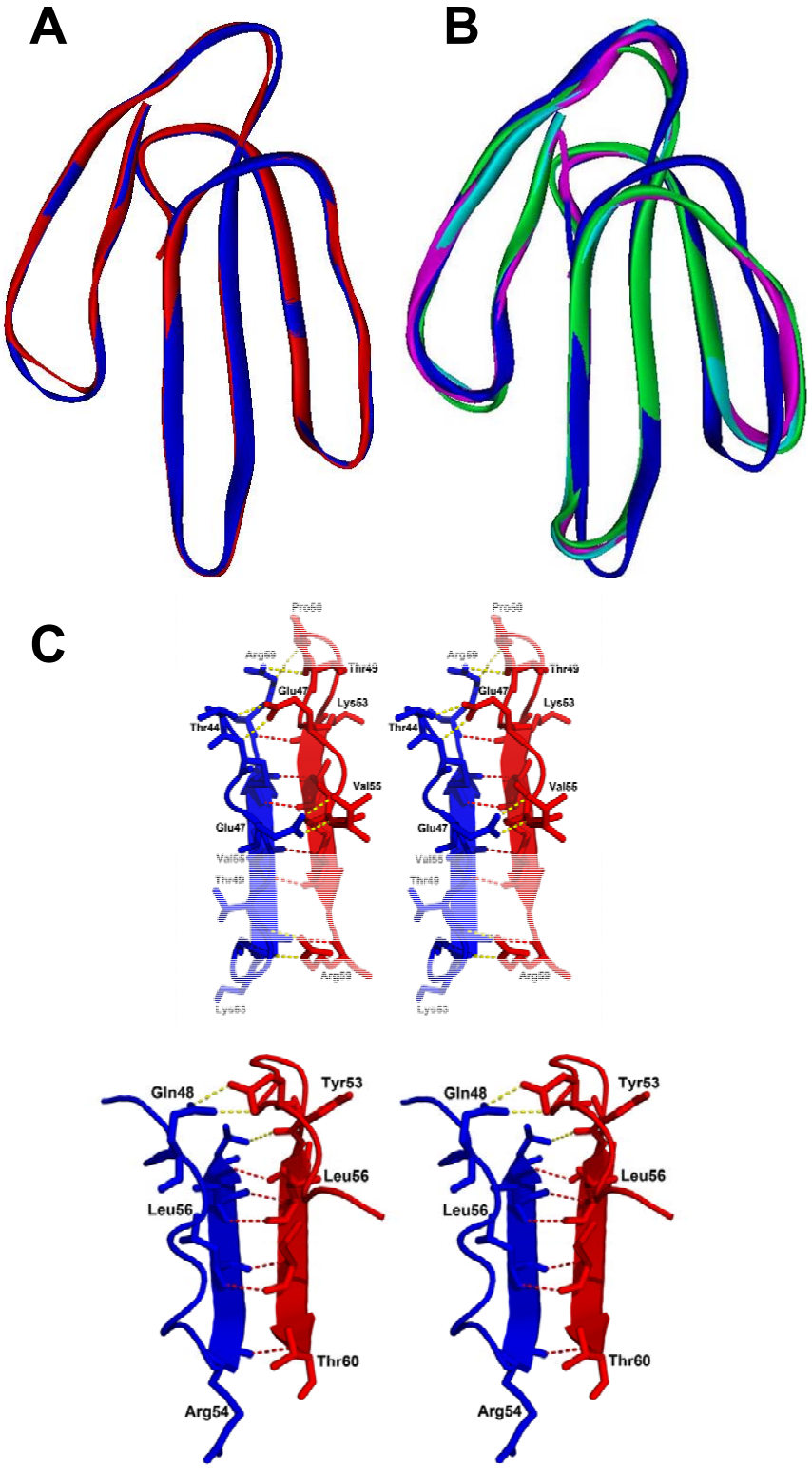

Figure 8